The following graphic will be used for the TOC:

Environmental Science & Technology

Article

pubs.acs.org/est

The Ozone–Climate Penalty: Past, Present, and Future

D. J. Rasmussen,[†,§] Jianlin Hu,[†] Abdullah Mahmud,[‡,§] and Michael J. Kleeman*[,†]

[†]Department of Civil and Environmental Engineering, University of California Davis, Davis, California 95616, Unites States

[‡]Department of Civil and Environmental Engineering, Portland State University, Portland, Oregon 97207, Unites States

Supporting Information

ABSTRACT: Climate change is expected to increase global mean temperatures leading to higher tropospheric ozone (O_3) concentrations in already polluted regions, potentially eroding the benefits of expensive emission controls. The magnitude of the "O_3–climate penalty" has generally decreased over the past three decades, which makes future predictions for climate impacts on air quality uncertain. Researchers attribute historical reductions in the O_3–climate penalty to reductions in NO_x emissions but have so far not extended this theory into a quantitative prediction for future effects. Here, we show that a three-dimensional air quality model can be used to map the behavior of the O_3–climate penalty under varying NO_x and VOC emissions in both NO_x-limited and NO_x-saturated conditions in Central and Southern California, respectively. Simulations suggest that the planned emissions control program for O_3 precursors will not diminish the O_3–climate penalty to zero as some observational studies might imply. The results further demonstrate that in a NO_x-limited air basin, NO_x control strategies alone are sufficient to both decrease the O_3–climate penalty and mitigate O_3 pollution, while in a NO_x-saturated air basin, a modified emissions control plan that carefully chooses reductions in both NO_x and VOC emissions may be necessary to eliminate the O_3–climate penalty while simultaneously reducing base case O_3 concentrations to desired levels. Additional modeling is needed to determine the behavior of the O_3–climate penalty as NO_x and VOC emissions evolve in other regions.

INTRODUCTION

Surface ozone (O_3) is a secondary pollutant produced by the photochemical oxidation of CO and/or volatile organic compounds (VOCs) by the hydroxyl radical ($^{\bullet}HO$) in the presence of oxides of nitrogen ($NO_x \equiv NO_2 + NO$). Model perturbation studies have identified temperature as the most important weather variable affecting surface O_3 concentrations in polluted regions.[1−5] These findings have been validated against observations on multiple time scales that have shown strong correlations between temperature and O_3 concentrations in excess of about 60 ppb.[6−8] California is home to seven of the top ten most heavily O_3 polluted metropolitan areas in the United States ,[9] despite the dramatic reductions of NO_x and VOC precursor emissions over the past three decades.[3−6,10−12] A warming climate is expected to exacerbate surface O_3 in California's two major air basins: South Coast Air Basin (SoCAB) and San Joaquin Valley (SJV). Median surface temperatures during the O_3 season over western North America, including the SoCAB and SJV, are projected to warm between +1 to +5 K by the end of the 21st century.[13] These temperature increases may counter the benefits from pollution control strategies used in an effort to meet established air quality standards, resulting in a "climate penalty".[14,15]

In this study, the sensitivity of O_3 to temperature and NO_x and VOC emissions is calculated in both NO_x-saturated and NO_x-limited conditions with a reactive chemical transport model during two historical severe weekday pollution episodes in California: the SoCAB during September 7–9, 1993 (NO_x-saturated)[16,17] and the SJV during July 25–27, 2005 (NO_x-limited). Historical episodes are used for the base case analysis to enable the study of O_3-temperature relationships over a period spanning the past two decades to future conditions over which NO_x and VOC emissions have evolved. The results in this study are presented as an O_3 isopleth diagram that simultaneously describes the maximum concentration (ppb) and sensitivity to temperature (ppb K^{-1}) of surface O_3 under specified NO_x and VOC emissions.[18] This map of O_3–temperature relationships is compared to historical trends for validation and then projected forward to predict climate impacts on future O_3 pollution.

THE O_3–CLIMATE PENALTY

Varying definitions of the O_3–climate penalty have been presented in the literature. Wu et al. consider the climate penalty to represent either the additional decreases in NO_x emissions to counter any climate driven increase in O_3 (assuming NO_x is the limiting precursor) or the reduced benefits of emissions controls

Received: August 2, 2013
Revised: October 15, 2013
Accepted: November 4, 2013

   dx.doi.org/10.1021/es403446m | Environ. Sci. Technol. XXXX, XXX, XXX–XXX

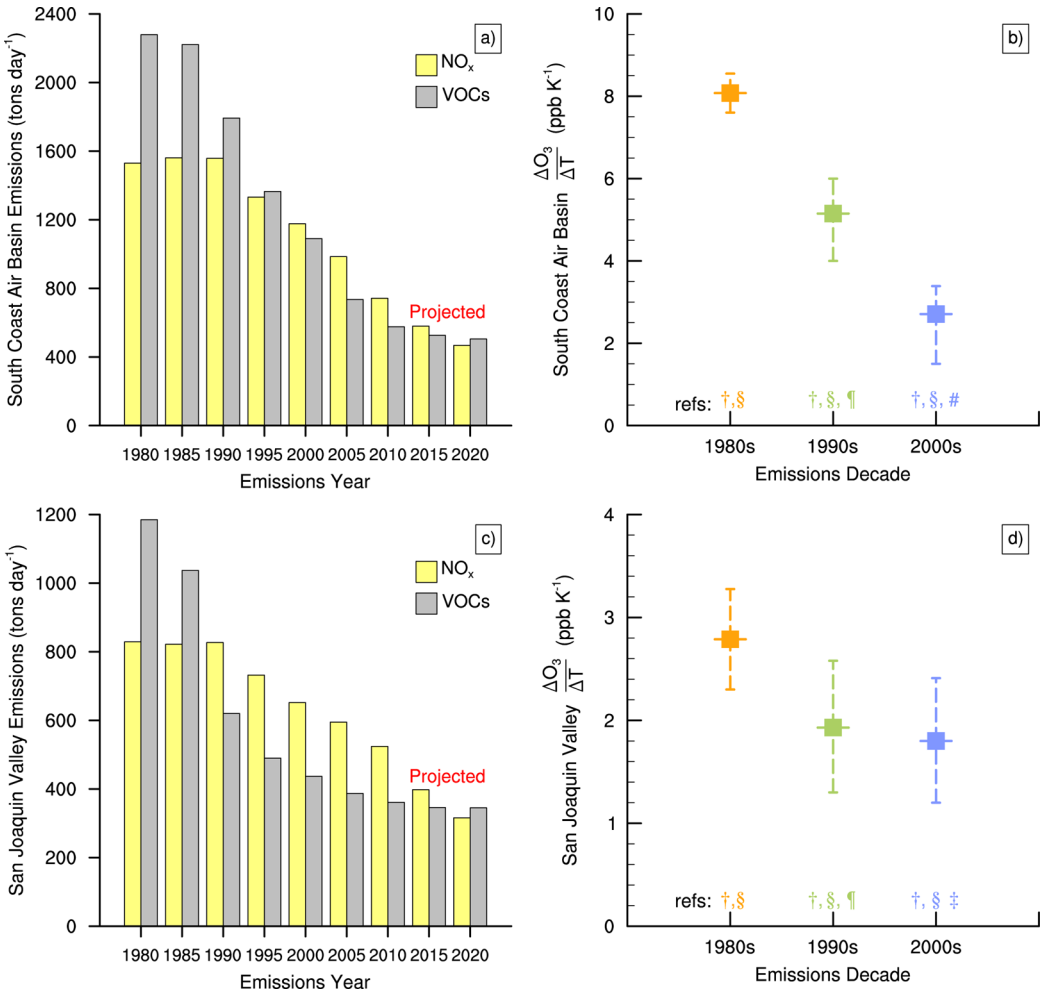

Figure 1. (a) Historical and projected average daily anthropogenic NO_x (yellow) and VOC (gray) emissions (tons day^{-1}) vs emissions year for the South Coast Air Basin and (b) the observed decadal trend in the O_3–climate penalty for the Southern California Air Basin attributed to emissions changes during the 1980s (orange), the 1990s (green), and the 2000s (blue). Dashed lines give the range of both observed and modeled O_3–climate penalty values in the South Coast Air Basin from the literature; solid squares are the mean O_3–climate penalty calculated from values given in the literature. Symbols beneath each range correspond to literature references: † is Mahmud et al.[6] (statistical down-scaling based on measured trends), § is Steiner et al.[8] (observations), ¶ is Kleeman[3] (model perturbation), # is Millstein and Harley[4] (model perturbation), and ‡ is Steiner et al.[5] (model perturbation); (c) as for (a) but for the San Joaquin Valley; (d) as for (b) but for the San Joaquin Valley.

due to the increase in O_3 due to a warmer climate.[15] Bloomer et al. calculate the "ozone–climate penalty factor" as the slope of the best fit line between long-term observational measurements of O_3 and temperature.[19] Other studies utilizing air quality models quantified the change in O_3 due to a prescribed temperature perturbation but did not refer to this sensitivity as a "climate penalty".[3,4,6] Here, we employ the temperature perturbation approach and refer to the direct increase in O_3 concentrations due to increasing temperatures (ppb K^{-1}) as the "O_3–climate penalty" or "climate penalty". Previous work has shown the past and present climate penalty to be highly varied in space and time due to differing chemical and meteorological environments that influence O_3 formation.[3,4,6,8,19] The aggregate effects that make up this relationship (the total derivative, $d[O_3]/dT$) are thought to include at least three components

$$\frac{d[O_3]}{dT} = \frac{\partial[O_3]}{\partial[\text{stagnation}]} \times \frac{d[\text{stagnation}]}{dT} + \frac{\partial[O_3]}{\partial[\text{reaction}]} \times \frac{d[\text{reaction}]}{dT} + \frac{\partial[O_3]}{\partial[\text{BVOC}]} \times \frac{d[\text{BVOC}]}{dT} + \ldots$$

The first term accounts for the association of warm temperatures with stagnant air masses that facilitate the accumulation of O_3 precursor species.[20] The second term accounts for the increase in chemical reaction rates for different species, including the thermal decomposition of alkyl nitrates (AN) and subspecies peroxyacetylnitrate (PAN), reservoirs for both NO_x and HO_x at low temperatures.[7] The third term accounts for temperature dependent variations in biogenic emissions of VOCs (BVOCs), which act as a significant source of precursors for O_3 formation under high-NO_x conditions and tend to increase with temperature for many species.[21,22] The ellipsis indicates several additional contributing temperature-dependent processes of varying sign that may not be dominant

dx.doi.org/10.1021/es403446m | Environ. Sci. Technol. XXXX, XXX, XXX–XXX

under the assumptions of the current study, including wildfires in the western United States[23] and humidity in the Mid-Atlantic [24] (see Table 1 in ref 25 for a comprehensive list). Model perturbation studies resolve the climate penalty partial derivatives, while observations ascertain the total derivative. Extrapolation of present day O_3–temperature relationships to future climate to estimate changes in O_3 air quality assumes invariable emission rates and ignores complex chemistry–climate interactions.[14,25,26]

HISTORICAL TREND IN O_3–CLIMATE PENALTY IN CALIFORNIA

Figure 1 shows the trend in average daily NO_x and VOC emissions in the SoCAB and the SJV, along with the corresponding decadal trend in the climate penalty from previous model perturbation and observational studies. The climate penalty is strongly correlated with NO_x and VOC emissions in both the SoCAB and the SJV. From 1980 to 2010, average daily emissions of NO_x and VOCs in the SoCAB decreased roughly 2- and 4-fold, respectively; in the SJV, NO_x and VOC emissions decreased by a factor of 1.5- and 3-fold, respectively.[27] The dramatic decrease in these emissions reflects the success of California's statewide emission control programs. Over this same period, the mean value of climate penalty in the SoCAB decreased from +8.0 ppb K^{-1} in the 1980s to a present day value of +2.7 ppb K^{-1}, while the climate penalty in the SJV decreased from a value of +2.8 ppb K^{-1} in the 1980s to a current value of +1.8 ppb K^{-1}.[3,4,6,8,19] Similar NO_x–climate penalty trends have been observed elsewhere. In the eastern United States, a 43% reduction in power plant NO_x emissions between 1995 and 2002 was shown to correspond to a 1.0 ppb K^{-1} decrease in the O_3–climate penalty.[19,28] Over the next decade, emissions of NO_x and VOCs are expected to continue to decrease in both the SoCAB and the SJV raising the following question: Will the O_3–climate penalty effectively diminish to zero, or does a particular emissions strategy exist that minimizes the O_3–climate penalty?

METHODS

Model Description. The UC-Davis-California Institute of Technology (UCD-CIT) air quality model is a 3D Eulerian photochemical model that simulates reactive chemical transport in the atmosphere and predicts the concentration of both primary and secondary pollutants in the gas and particle phase. Relevant chemical reactions are modeled with the SAPRC11 mechanism.[29] A coupled online UV radiative extinction calculation accounts for the scattering and absorption of light due to high airborne particulate matter concentrations to give a more accurate representation of actinic flux. A more thorough description of the UCD-CIT airshed model and its evolution has been presented previously.[17,30–33]

Because of variations in the physical characteristics of each air basin, different model configurations were used to simulate each pollution episode. The horizontal resolution used in the SoCAB simulations was 5 km × 5 km. The vertical domain was divided into 5 levels (thicknesses of 38.5, 115.5, 154, 363, and 429 m), extending from the surface to 1.1 km above ground. This relatively shallow model depth is only appropriate in well-defined air basins, such as the SoCAB, where pollutants have a residence time of only a few days. The horizontal resolution in the SJV simulations was 8 km × 8 km, and the vertical distance from the surface to 5 km above ground was divided into 16 levels (the surface to 1.1 km above ground for the SJV simulations is comprised of 11 levels). In the SoCAB, hourly 2D and 3D meteorological fields (temperature, absolute humidity, wind speed and direction, and solar intensity) were interpolated from observations using the method described by refs 34 and 35, while the SJV simulations used hourly meteorological fields generated over California at 4 km × 4 km horizontal resolution with the Weather Research and Forecasting model (WRF) v3.4,[36] driven by the North American Regional Reanalysis (NARR).[37] Four-dimensional data assimilation (FDDA) is further used to nudge WRF model estimates closer to observed conditions. The WRF meteorological fields were averaged to 8 km × 8 km to reduce model simulation times. Previous studies have shown these configurations to well reproduce measured pollutant concentrations.[17,38]

The base case emission inventories for the SoCAB and SJV episodes were obtained from the South Coast Air Quality Management District (SCAQMD) and the California Air Resources Board (ARB) and are summarized in refs 39 and 40, respectively. Boundary conditions at the western edge of each modeling domain were based on measured background concentrations of pollutants that are transported to California[41,42] and remained constant while emission perturbations were applied. Biogenic emissions were generated at 8 km × 8 km spatial resolution using the Biogenic Emission Inventory Geographic Information System (BEIGIS) model.[43] A year 2000 land-use pattern generated by the moderate-resolution imaging spectroradiometer (MODIS) satellite is used to determine vegetation types and leaf area indices. Hourly averaged surface air temperature and shortwave radiation from the meteorology are used to calculate emissions of isoprene, monoterpenes, and 2-methyl-3-buten-2-ol (MBO).[21,22] In the SJV, livestock feed VOC emissions were estimated using the method described by ref 44 and are mapped to the spatial distribution of livestock ammonia emissions. Predicted O_3 concentrations for both pollution episodes in this study had performance statistics that met U.S. Environmental Protection Agency (EPA) guidance for air quality models.[45]

Calculating the O_3–Climate Penalty. To generate an O_3 isopleth diagram, the episode base case emissions of NO_x and anthropogenic VOCs were uniformly scaled up (more emissions) or down (less emissions) to represent a hypothetical range of pollution control strategies in each air basin. Here, the air quality model explicitly simulates 121 and 64 NO_x and VOC emissions scenarios in the SoCAB and SJV, respectively. These simulations are then repeated after applying a temperature perturbation for a total of 370 model runs. In this study, a spatially uniform temperature perturbation was applied to every hour during both multi-day pollution events to calculate a value of the climate penalty at each NO_x and VOC emissions point. This technique explores the O_3–climate penalty under base case conditions to better understand important relationships between emissions and climate. Further work would be required to account for detailed future emissions trends and projected climate patterns if the effects of these secondary factors on future O_3–climate penalties are of interest.

The O_3–climate penalty was calculated as the difference between the O_3 concentrations predicted with the base case temperature profile and the base case temperature profile plus a −5 K perturbation divided by the magnitude of the temperature perturbation (ppb K^{-1}). The magnitude of the perturbation is arbitrary and is not intended to reflect a projection of future temperature change. Previous work has shown the O_3–climate penalty is not strongly sensitive to the absolute magnitude of the

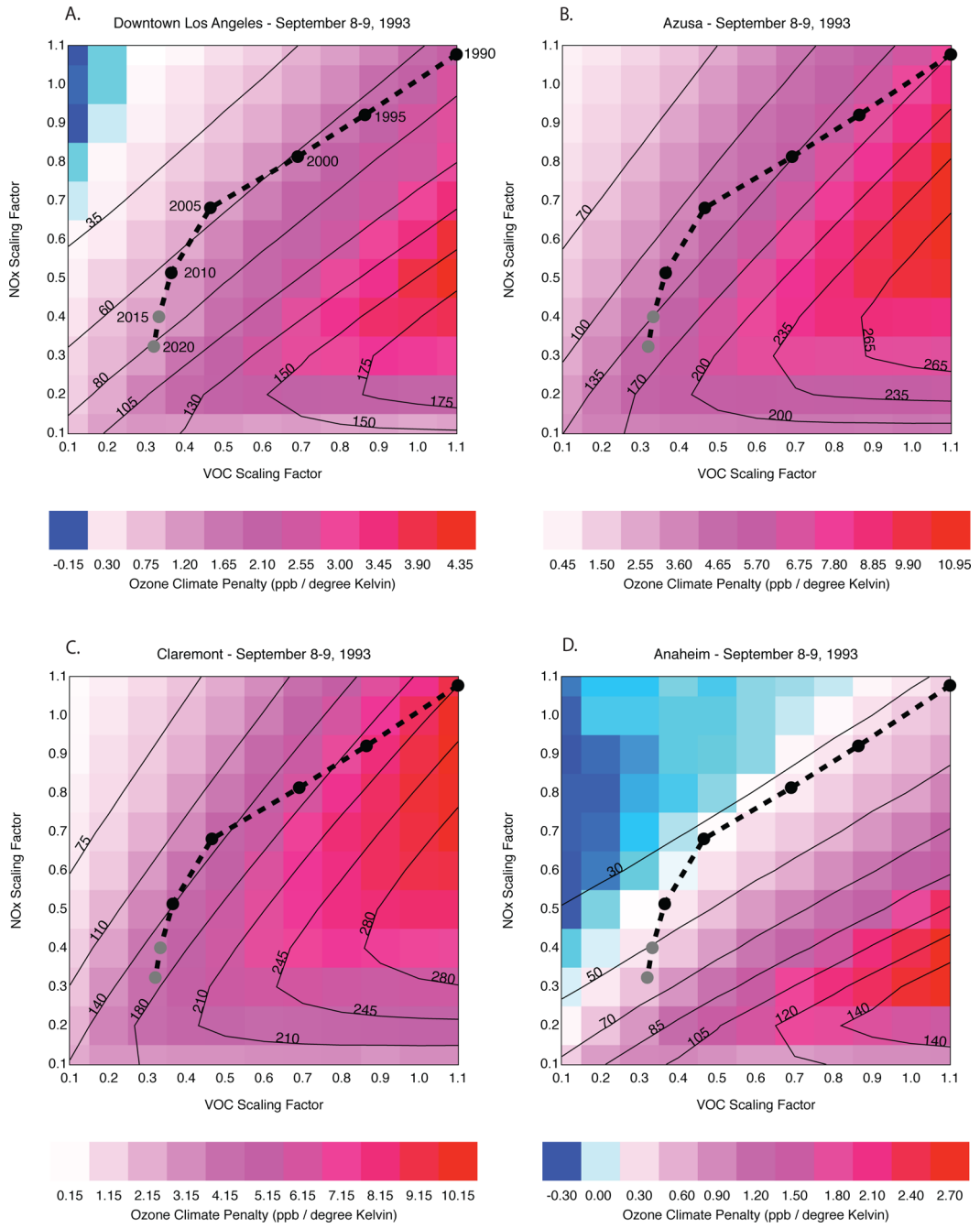

Figure 2. Isopleths of 8 h average O_3 (ppb)(solid black lines) and O_3–climate penalty (ppb K^{-1}) (colors) generated from a −5 K temperature perturbation for (a) Downtown Los Angeles, (b) Azusa, (c) Claremont, and (d) Anaheim. All calculations are for the conditions on September 8–9, 1993. Estimated anthropogenic emissions trend relative to the 1993 base year is shown as a dashed black line. A different color scale is used for each panel.

temperature perturbation used.[3] A negative (rather than positive) temperature perturbation was chosen in the present study because maximum daily temperatures from the base case episodes were greater than 40 °C and the contributions to $d[O_3]/dT$ from PAN decomposition and isoprene emissions have been shown to diminish at temperatures >39 °C.[8] Not fully accounting for these contributions could lead to an under prediction of the base case O_3 sensitivity to temperature. The negative perturbation produces temperatures that are more in line with historical temperature ranges and therefore yields values of $\partial[O_3]/\partial T$ that are more directly comparable to $d[O_3]/dT$ calculated from long-term measurements of O_3 and temperature.[6,8,19,46]

In this study, the temperature perturbation affects chemical kinetic reaction rates and biogenic emissions of isoprene, monoterpenes, and MBO.[21,22] The temperature perturbation does not alter the evaporation of anthropogenic VOCs [47] or the emission rate of soil NO_x and is uncoupled from temperature dependent meteorological variables such as mixed layer depth, solar insolation, wind speed and wind direction; model perturbation studies have shown that mixed layer depth has weak positive and negative effects on O_3 concentrations in polluted regions.[1,3] Temperature driven changes to atmospheric

dx.doi.org/10.1021/es403446m | Environ. Sci. Technol. XXXX, XXX, XXX–XXX

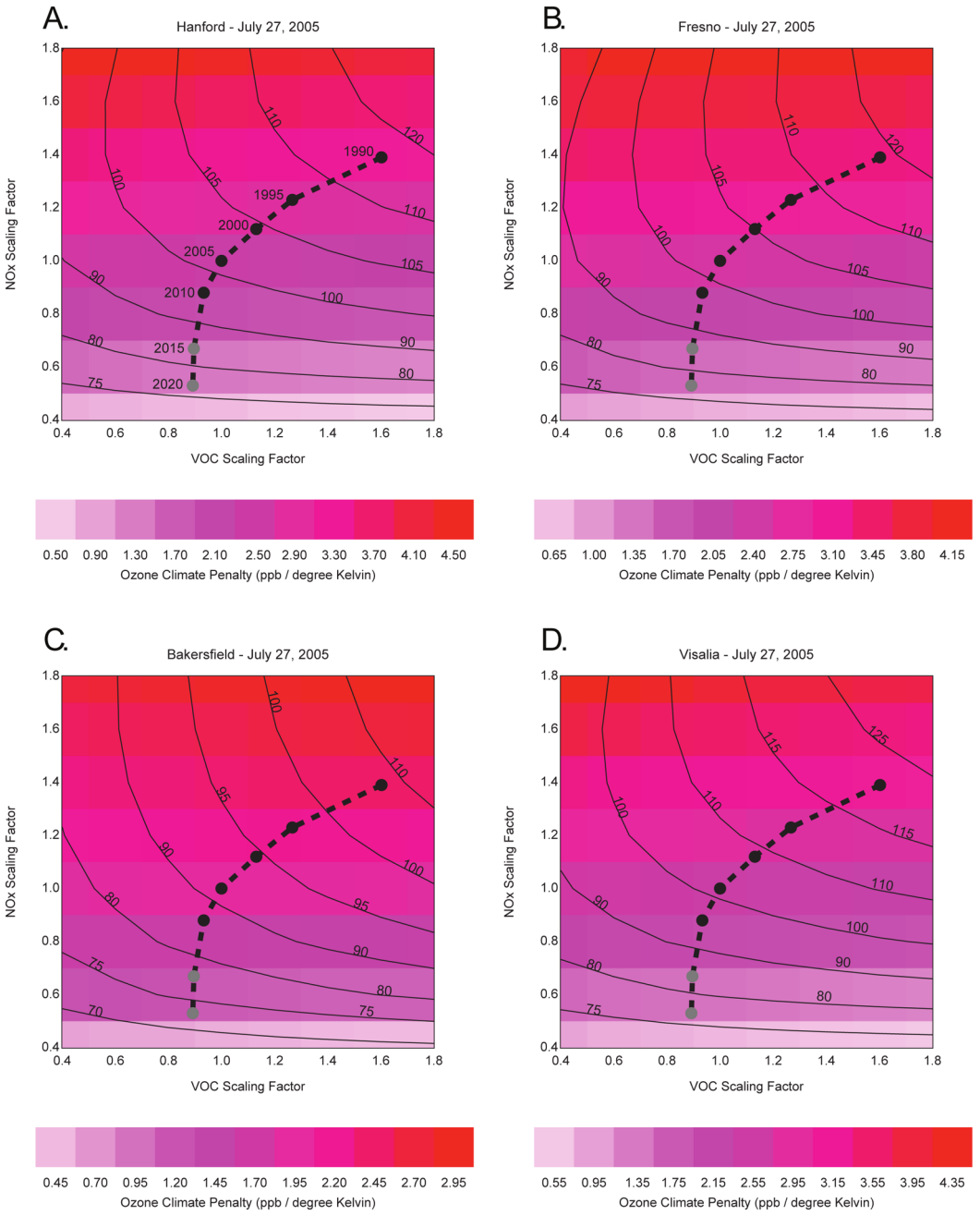

Figure 3. Isopleths of 8 h average O_3 (ppb)(solid black lines) and O_3–climate penalty (ppb K^{-1}) (colors) generated from a −5 K temperature perturbation for (a) Hanford, (b) Fresno, (c) Bakersfield, and (d) Visalia. All calculations are for the conditions on July 27, 2005. Estimated anthropogenic emissions trend relative to the 2005 base year is shown as a dashed black line. A different color scale is used for each panel.

circulation are not considered and could be important in defining the exact meteorological characteristics of peak O_3 episodes. Vegetation and land use data remain constant.

The Clausius–Clapeyron relation predicts exponential increases in the atmosphere's capacity to hold water vapor with increasing temperature. Increases in water vapor can lead to greater HO_x production that may affect O_3 formation differently depending on the region and the atmospheric conditions.[1,2,4,48] The temperature perturbations applied in the current study were coupled with different assumptions about humidity for each air basin depending on their geographical features. The majority of the SoCAB is close to the Pacific Ocean where an unlimited water reservoir maintains an approximately constant relative humidity (RH) with increasing temperature. The RH was therefore held constant in the SoCAB when temperature was perturbed. In the SJV, the supply of moisture is limited, and it was therefore assumed that absolute humidity would remain constant with increasing temperature, leading to a decrease in RH. Additional SJV modeling simulations that assumed constant RH resulted in O_3–climate penalty values nearly identical to those that fixed absolute humidity.

RESULTS AND DISCUSSION

Decreases in NO_x and VOC Emissions and the O_3–Climate Penalty Response. Isopleths of 8 h average O_3 (10:00–18:00 LDT) (ppb) and O_3–climate penalty (ppb K^{-1}) for NO_x and VOC emissions rates relative to conditions on September 8–9, 1993 are shown in Figure 2 at Downtown Los

dx.doi.org/10.1021/es403446m | Environ. Sci. Technol. XXXX, XXX, XXX–XXX

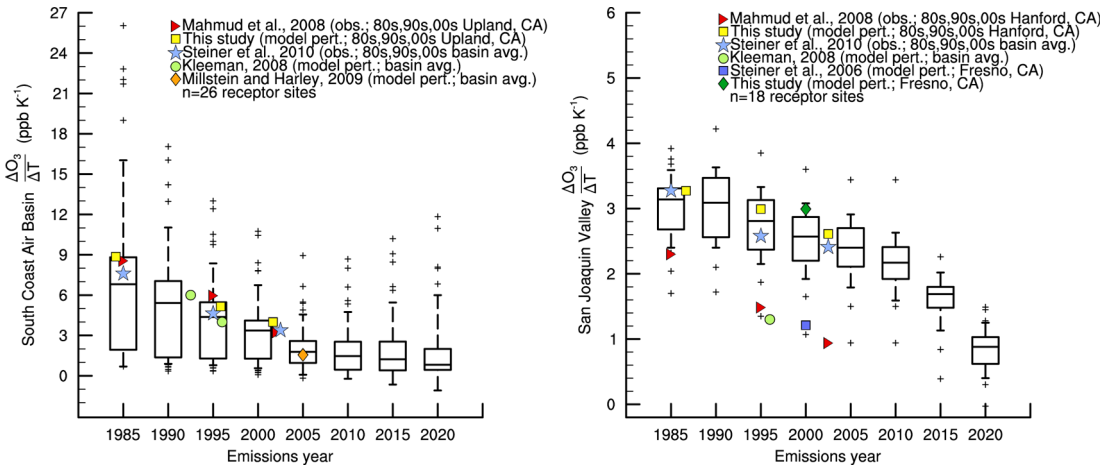

Figure 4. Historical (colored markers) and modeled O_3–climate penalty (ppb K^{-1}) for emissions years from 1985 to 2020 for the South Coast Air Basin (SoCAB) (left) and the San Joaquin Valley Air Basin (SJV) (right). The box-and-whisker plots (mean minus the standard deviation, 25th, 50th, 75th, and mean plus the standard deviation) give statistics of the modeled O_3–climate penalty at 26 urban receptors in the South Coast Air Basin and at 18 urban receptors in the San Joaquin Valley (Figure S1, Supporting Information). Values greater or less than the mean ± the standard deviation are shown as crosses. All modeled calculations are for the conditions on September 8–9, 1993 (SoCAB) and July 27, 2005 (SJV).

Angeles, Azusa, Claremont, and Anaheim in the SoCAB. Ozone isopleth diagrams generated for Visalia, Fresno, Hanford, and Bakersfield in the SJV for conditions on July 27, 2005 are shown in Figure 3. The SoCAB is an urban environment that is NO_x-saturated during weekdays,[49] while both the SJV and the eastern United States are predominantly NO_x-limited at all times.[50] Each isopleth shows the modeled base case O_3 concentration under a particular set of NO_x and VOC emissions rates with the same meteorology. In these simulations, NO_x is emitted from both soil and anthropogenic sources and VOC is emitted from anthropogenic and natural sources. For both air basins, NO_x and only anthropogenic VOC emissions are scaled. The scaling factors are the fraction of NO_x and VOC emissions relative to the base years. The base year for the SJV episode is 2005, and the base year for the SoCAB episode is 1993. Base years have a scaling factor of 1. The range of scaling factors was chosen to capture the range of both historical and projected emissions.

The colors overlaid on each O_3 isopleth diagram in Figures 2 and 3 show the magnitude of O_3–climate penalty (ppb K^{-1}). The maximum in the O_3–climate penalty occurs at a NO_x emission level slightly greater than that which produces the maximum O_3 under the base case temperature simulation and at the highest VOC emission rates. This is coincident with the "O_3 isopleth ridge", or the line of maximum O_3 formation. The minimum in O_3–climate penalty occurs in conditions that are appreciably NO_x-saturated. The simulations here suggest that when NO_x emissions are much greater than VOC emissions, the O_3–climate penalty may become strongly negative (i.e., a climate "benefit") at Downtown LA and Anaheim (−0.1 to −0.4 ppb K^{-1}) (O_3 decreases with increasing temperature), suggestive of O_3 titration by NO from further NO_x-saturation that results from the thermal decomposition of PAN at hotter temperatures.[7]

The historical and projected trend (1990—2020) in average daily anthropogenic NO_x and VOC emissions rates, relative to the respective base case inventory, is drawn on each isopleth diagram as black (historical) and gray (projected) dots connected by a dashed black line, taken together to constitute an emissions "trajectory". Receptors in each air basin are assumed to experience an equivalent rate of NO_x and VOC emissions reductions. The O_3 values along the NO_x–VOC emissions trajectory are an estimate of the maximum amount of O_3 pollution that could be formed during a severe pollution event with similar meteorology. Substantially NO_x-saturated conditions are not predicted by the emissions trajectory at any of the SoCAB or SJV receptors over the next decade (Figures 2 and 3).

In both air basins, the O_3 isopleth diagrams suggest that NO_x and VOC emission reductions between 1990 and 2010 have been effective at abating O_3 during weekday severe pollution events, especially in eastern LA and the SJV, confirming previous findings.[11,27] Reductions in O_3 in the SoCAB were accomplished through reductions in emissions of both NO_x and VOCs. Figure 2 shows that reductions in NO_x emissions alone over this 20-year period would have increased O_3 concentrations in the SoCAB. Little change in O_3 is seen at both Anaheim and Downtown LA (Figure 2a,d) because reductions in NO_x and VOC emissions produce a trajectory that stays within a zone of approximately constant O_3. In the SJV, reductions in O_3 have primarily occurred through reductions in NO_x emissions.

Over the next decade, the ARB projects that NO_x and VOC emissions will continue to decrease in both air basins, with NO_x emissions declining more rapidly. Projections for the SoCAB indicate that this emissions trajectory may not be optimal, with slight increases in O_3 concentrations (+20 to +30 ppb under the meteorological conditions studied). This result is consistent with findings from other investigators; Fujita et al. find that reductions in NO_x emissions without concurrent VOC emission reductions over the next decade will cause O_3 to increase in central portions of the SoCAB during weekdays.[10] No such effect is predicted for the SJV in the present study; the O_3 isopleths for the SJV predict continued decreases in O_3 over the next decade under meteorological conditions conducive to O_3 formation (Figure 3).

The historical and projected trend in the O_3–climate penalty can be inferred from the NO_x–VOC emission trajectory on the isopleths (Figures 2 and 3). Both NO_x and VOC emissions appear to play a role in determining the O_3–climate penalty in the SoCAB, contrary to previous findings that suggest NO_x emissions are the primary explanatory variable in the observed decreasing trend in the O_3–climate penalty.[19] Reducing NO_x emissions, primarily emitted as nitric oxide (NO), in a NO_x-saturated environment can exacerbate O_3 pollution by both decreasing O_3 loss by NO titration and increasing the ratio of VOCs to NO_x, favoring peroxy (HO_2) and alkylperoxy (RO_2)

dx.doi.org/10.1021/es403446m | Environ. Sci. Technol. XXXX, XXX, XXX–XXX

formation, both of which propagate the chain reaction mechanism that produces O_3 in the troposphere.[51] While NO_x emission controls may be effective at decreasing the O_3–climate penalty in the NO_x-limited eastern United States and SJV,[19,50] the results of the current study suggest that further decreases in VOC emissions over the next decade in the SoCAB (NO_x-saturated) may be beneficial to reducing base case O_3 pollution and may additionally be effective at minimizing the O_3–climate penalty.

Future Trend in the O_3–Climate Penalty and Implications. The O_3 isopleth diagrams illustrate climate penalty–emissions relationships at individual receptor sites but do not readily facilitate an air basin-wide assessment of historical and projected trends in the O_3–climate penalty along the emissions trajectory. To characterize an air basin-wide climate penalty, we use 18 urban receptor sites in the SJV and 26 urban receptor sites in the SoCAB. The location of these receptors are shown in Figure S1 of the Supporting Information and are analogous to the receptor sites that are used by ref 8. Figure 4 shows the modeled historical (1985–2010) and projected (2015–2020) trend in O_3–climate penalty (ppb K^{-1}) at these receptor sites in the SoCAB (left) and the SJV (right). Modeled results are presented as box-and-whisker plots (25th, median, and 75th percentiles) where the whiskers are the mean (not shown) ± the standard deviation. Values outside of the whiskers are plotted as crosses. Historical values of the O_3–climate penalty from the literature (as both air basin averages and at individual receptors) are drawn as solid black symbols. Values given by ref 8 are decadal air basin averages constructed from long-term measurements and likely capture the full O_3–temperature relationship.

The observed trend of the O_3–climate penalty from all literature sources are generally well reproduced by the air quality model using the meteorology from severe pollution events that are characterized by very hot surface temperatures (r^2 = 0.98 in the SoCAB; r^2 = 0.69 in the SJV). The median model prediction is systematically lower than the measured climate penalty from ref 8 by at most 0.8 ppb K^{-1} in the SoCAB over the past three decades but is reproduced to within ±0.3 ppb K^{-1} in the SJV from the 1990s to the 2000s. In the SJV, site-by-site differences in the O_3–climate penalty are more pronounced (±1 ppb K^{-1}), including between the current and past model perturbation studies[3,8] and may reflect differing assumptions therein. Differences between modeled and observed values may reflect emissions sector changes (i.e., changes to VOC reactivity [52]) during the past three decades that are not captured using the uniform emissions scaling approach employed here or other contributions that are not captured with the simple temperature perturbation approach that only affects kinetic rate constants, biogenic emission rates, and water vapor concentrations in a representative episode. For example, calculation of the O_3–climate penalty from long-term modeled O_3 and surface temperature may yield different sensitivities than those derived from a single severe pollution event as some contributing components of the full O_3–temperature relationship may be driven by intraseasonal weather patterns and events. The choice of biogenic emissions models and chemical mechanisms may also influence the predicted climate penalty. The sensitivity of the results to these modeling options should be investigated in future work.

The range of climate penalties at receptors in the SoCAB in 1985 varies by about a factor of 30, +0.7 ppb K^{-1} to +26.2 ppb K^{-1}, a substantially wider range of variability compared to the SJV, +0.6 ppb K^{-1} to +3.9 ppb K^{-1}. Receptors east of Los Angeles that are adjacent to the San Gabriel Mountains (a large source of biogenic VOCs) have the largest climate penalties through out the simulation period (1985–2020) (Figure S2a, Supporting Information). These sites are likely sensitive to increased biogenic VOC emissions through rises in temperature. The central and coastal receptors in the SoCAB consistently have the lowest climate penalty as they may be saturated with fresh NO emissions that titrate O_3. While the future median O_3–climate penalty is projected to decrease steadily in both air basins, some receptors in the SoCAB near the San Gabriel Mountains (e.g., Azusa and Claremont, Figure 2b,c) are expected to experience a rise in the climate penalty due to the strengthening sensitivity of O_3 to strong biogenic emissions in a region where NO_x decreases much more rapidly than VOC emissions. The 2020 median O_3–climate penalty is projected to be +0.8 ppb K^{-1} in the SoCAB (basin-wide range of −0.8 ppb K^{-1} to +11.8 ppb K^{-1}) and +0.9 ppb K^{-1} in the SJV (basin-wide range of 0.0 ppb K^{-1} to +1.5 ppb K^{-1}), suggesting under the projected emissions pathway that increases in temperature due to climate change may continue to have deleterious effects on O_3 control programs. Although average daily NO_x and VOC emissions are projected to decrease 37% and 12%, respectively, over the next decade in the SoCAB,[27] potential concomitant anthropogenic VOC emissions reductions may be beneficial to reduce both base case O_3 and to further diminish the O_3–climate penalty.

In NO_x-limited regions such as the SJV and the eastern United States, continued decreases in NO_x emissions are anticipated and may continue to lower the O_3–climate penalty. The exact O_3–temperature relationship at other locations should be evaluated for a representative episode of interest (peak or average) using an appropriate reference year (historical or present day). Future studies should also account for climate-driven changes to atmospheric circulation, changes in land use, choice of boundary conditions that reflect changes to long-range transport of pollutants, and scaling individual emissions sectors to accurately reflect emission control targets.

■ ASSOCIATED CONTENT

Supporting Information

Figures showing the location of the ozone receptors used in this study and model results for each air basin showing the spatial distribution of the ozone–climate penalty. This material is available free of charge via the Internet at http://pubs.acs.org.

■ AUTHOR INFORMATION

Corresponding Author

*E-mail: mjkleeman@ucdavis.edu. Phone: +1 (530) 752-8386. Fax: +1 (530) 752-7872.

Present Address

§ D.J.R. and A.M.: California Air Resources Board, Sacramento, California 95814, United States).

Notes

The authors declare no competing financial interest.

■ ACKNOWLEDGMENTS

Research reported in this publication was partially supported by the National Institutes of Health under Award Number ES020237. The content is solely the responsibility of the authors and does not necessarily represent the official views of the National Institutes of Health. We thank M. Hixson for data processing tools to prepare the model inputs. We acknowledge three anonymous reviewers and C. Anastasio, C. Cappa (UC-

Davis), J. Chen, and A. Kaduwela (CARB) for providing comments on earlier versions of the manuscript.

REFERENCES

(1) Aw, J.; Kleeman, M. J. Evaluating the first-order effect of intraannual temperature variability on urban air pollution. *J. Geophys. Res.-Atmos.* **2003**, *108*.

(2) Dawson, J. P.; Adams, P. J.; Pandis, S. N. Sensitivity of ozone to summertime climate in the eastern USA: A modeling case study. *Atmos. Environ.* **2007**, *41*, 1494−1511.

(3) Kleeman, M. J. A preliminary assessment of the sensitivity of air quality in California to global change. *Climatic Change* **2008**, *87*, S273−S292.

(4) Millstein, D. E.; Harley, R. A. Impact of climate change on photochemical air pollution in Southern California. *Atmos. Chem. Phys.* **2009**, *9*, 3745−3754.

(5) Steiner, A. L.; Tonse, S.; Cohen, R. C.; Goldstein, A. H.; Harley, R. A. Influence of future climate and emissions on regional air quality in California. *J. Geophys. Res.-Atmos.* **2006**, *111*, D18303.

(6) Mahmud, A.; Tyree, M.; Cayan, D.; Motallebi, N.; Kleeman, M. J. Statistical downscaling of climate change impacts on ozone concentrations in California. *J. Geophys. Res.-Atmos.* **2008**, *113*, D21103.

(7) Sillman, S.; Samson, F. J. Impact of temperature on oxidant photochemistry in urban, polluted rural and remote environments. *J. Geophys. Res.-Atmos.* **1995**, *100*, 11497−11508.

(8) Steiner, A. L.; Davis, A. J.; Sillman, S.; Owen, R. C.; Michalak, A. M.; Fiore, A. M. Observed suppression of ozone formation at extremely high temperatures due to chemical and biophysical feedbacks. *Proc. Natl. Acad. Sci. U.S.A.* **2010**, *107*, 19685−19690.

(9) State of the Air Report, 2013. American Lung Association. http://www.stateoftheair.org/2012/city-rankings/most-polluted-cities.html.

(10) Fujita, E. M.; Campbell, D. E.; Stockwell, W. R.; Lawson, D. R. Past and future ozone trends in California's South Coast air basin: Reconciliation of ambient measurements with past and projected emission inventories. *J. Air Waste Manage. Assoc.* **2013**, *63*, 54−69.

(11) Parrish, D. D.; Singh, H. B.; Molina, L.; Madronich, S. Air quality progress in North American megacities: A review. *Atmos. Environ.* **2011**, *45*, 7015−7025.

(12) Warneke, C.; de Gouw, J. A.; Holloway, J. S.; Peischl, J.; Ryerson, T. B.; Atlas, E.; Blake, D.; Trainer, M.; Parrish, D. D. Multiyear trends in volatile organic compounds in Los Angeles, California: Five decades of decreasing emissions. *J. Geophys. Res.-Atmos.* **2012**, *117*.

(13) Chistensen, J.et al. In *Climate Change 2013: The Physical Science Basis. Contribution of Working Group I to the Fifth Assessment Report of the Intergovernmental Panel on Climate Change*; Fyfe, J., Kwon, W.-T., Trenberth, K., Wratt, D., Eds.; Cambridge University Press: Cambridge, U.K., 2014.

(14) Jacob, D. J.; Winner, D. A. Effect of climate change on air quality. *Atmos. Environ.* **2009**, *43*, 51−63.

(15) Wu, S.; Mickley, L. J.; Leibensperger, E. M.; Jacob, D. J.; Rind, D.; Streets, D. G. Effects of 2000−2050 global change on ozone air quality in the United States. *J. Geophys. Res.-Atmos.* **2008**, *113*, D06302.

(16) Fraser, M. P.; Kleeman, M. J.; Schauer, J. J.; Cass, G. R. Modeling the atmospheric concentrations of individual gas-phase and particle-phase organic compounds. *Environ. Sci. Technol.* **2000**, *34*, 1302−1312.

(17) Ying, Q.; Fraser, M. P.; Griffin, R. J.; Chen, J.; Kleeman, M. J. Verification of a source-oriented externally mixed air quality model during a severe photochemical smog episode. *Atmos. Environ.* **2007**, *41*, 1521−1538.

(18) Sillman, S. The relation between ozone, NO_x and hydrocarbons in urban and polluted rural environments. *Atmos. Environ.* **1999**, *33*, 1821−1845.

(19) Bloomer, B. J.; Stehr, J. W.; Piety, C. A.; Salawitch, R. J.; Dickerson, R. R. Observed relationships of ozone air pollution with temperature and emissions. *Geophys. Res. Lett.* **2009**, *36*, L09803.

(20) Jacob, D. J.; Logan, J. A.; Yevich, R. M.; Gardner, G. M.; Spivakovsky, C. M.; Wofsy, S. C.; Munger, J. W.; Sillman, S.; Prather, M. J.; Rodgers, M. O.; Westberg, H.; Zimmerman, P. R. Simulation of summertime ozone over North America. *J. Geophys. Res.-Atmos.* **1993**, *98*, 14797−14816.

(21) Guenther, A. B.; Zimmerman, P. R.; Harley, P. C.; Monson, R. K.; Fall, R. Isoprene and monoterpene emission rate variability - model evaluations and sensitivity analyses. *J. Geophys. Res.-Atmos.* **1993**, *98*, 12609−12617.

(22) Harley, P.; Fridd-Stroud, V.; Greenberg, J.; Guenther, A.; Vasconcellos, P. Emission of 2-methyl-3-buten-2-ol by pines: A potentially large natural source of reactive carbon to the atmosphere. *J. Geophys. Res.-Atmos.* **1998**, *103*, 25479−25486.

(23) Pfister, G. G.; Wiedinmyer, C.; Emmons, L. K. Impacts of the fall 2007 California wildfires on surface ozone: Integrating local observations with global model simulations. *Geophys. Res. Lett.* **2008**, *35*.

(24) Camalier, L.; Cox, W.; Dolwick, P. The effects of meteorology on ozone in urban areas and their use in assessing ozone trends. *Atmos. Environ.* **2007**, *41*, 7127−7137.

(25) Fiore, A. M.; et al. Global air quality and climate. *Chem. Soc. Rev.* **2012**, *41*, 6663−6683.

(26) Weaver, C. P.; et al. A preliminary synthesis of modeled climate change impacts on U.S. regional ozone concentrations. *B. Am. Meteorol.* **2009**, *90*, 1843−1863.

(27) Cox, P.; Delao, A.; Komorniczak, A.; Weller, A. *The California Almanac of Emissions and Air Quality*, 2009 edition; California Evironmental Protection Agency: Sacramento, CA, 2009,

(28) Kim, S. W.; Heckel, A.; McKeen, S. A.; Frost, G. J.; Hsie, E. Y.; Trainer, M. K.; Richter, A.; Burrows, J. P.; Peckham, S. E.; Grell, G. A. Satellite-observed US power plant NO_x emission reductions and their impact on air quality. *Geophys. Res. Lett.* **2006**, *33*.

(29) Carter, W. P.; Heo, G. Development of revised *SAPRC* aromatics mechanisms. *Atmos. Environ.* **2013**, *77*, 404−414.

(30) Kleeman, M.; Cass, G. A 3D Eulerian source-oriented model for an externally mixed aerosol. *Environ. Sci. Technol.* **2001**, *35*, 4834−48.

(31) Kleeman, M. J.; Cass, G. R.; Eldering, A. Modeling the airborne particle complex as a source-oriented external mixture. *J. Geophys. Res.-Atmos.* **1997**, *102*, 21355−21372.

(32) McRae, G. J.; Goodin, W. R.; Seinfeld, J. H. Development of a second-generation mathematical model for Urban air pollution-I. Model formulation. *Atmos. Environ.* **1982**, *16*, 679−696.

(33) Mysliwiec, M. J.; Kleeman, M. J. Source apportionment of secondary airborne particulate matter in a polluted atmosphere. *Environ. Sci. Technol.* **2002**, *36*, 5376−5384.

(34) Goodin, W. R.; McRae, G. J.; Seinfeld, J. H. An objective analysis technique for constructing three-dimensional urban-scale wind fields. *J. Appl. Meteorol.* **1980**, *19*, 98−108.

(35) Goodin, W. R.; McRae, G. J.; Seinfeld, J. H. A comparison of interpolation methods for sparse data: Application to wind and concentration fields. *J. Appl. Meteorol.* **1979**, *18*, 761−771.

(36) Skamarock, W. C.; Klemp, J. B. A time-split nonhydrostatic atmospheric model for weather research and forecasting applications. *J. Comput. Phys.* **2008**, *227*, 3465−3485.

(37) Mesinger, F.; et al. North American regional reanalysis. *Bull. Am. Meteorol.* **2006**, *87*, 343−+.

(38) Hu, J.; Howard, C. J.; Mitloehner, F.; Green, P. G.; Kleeman, M. J. Mobile source and livestock feed contributions to regional ozone formation in Central California. *Environ. Sci. Technol.* **2012**, *46*, 2781−2789.

(39) Griffin, R. J.; Dabdub, D.; Kleeman, M. J.; Fraser, M. P.; Cass, G. R.; Seinfeld, J. H. Secondary organic aerosol. 3. Urban/regional scale model of size- and composition-resolved aerosols. *J. Geophys. Res.-Atmos.* **2002**, *107*.

(40) Ying, Q.; Lu, J.; Kaduwela, A.; Kleeman, M. J. Modeling air quality during the California Regional PM10/PM2.5 Air Quality Study (CPRAQS) using the UCD/CIT source oriented air quality model - part II. Regional source apportionment of primary airborne particulate matter. *Atmos. Environ.* **2008**, *42*, 8967−8978.

(41) Fraser, M. P.; Grosjean, D.; Grosjean, E.; Rasmussen, R. A.; Cass, G. R. Air quality model evaluation data for organics. 1. Bulk chemical composition and gas/particle distribution factors. *Environ. Sci. Technol.* **1996**, *30*, 1731−1743.

(42) Liang, J.; Horowitz, L. W.; Jacob, D. J.; Wang, Y.; Fiore, A. M.; Logan, J. A.; Gardner, G. M.; Munger, J. W. Seasonal budgets of reactive nitrogen species and ozone over the United States, and export fluxes to the global atmosphere. *J. Geophys. Res.-Atmos.* **1998**, *103*, 13435−13450.
(43) Scott, K. I.; Benjamin, M. T. Development of a biogenic volatile organic compounds emission inventory for the SCOS97-NARSTO domain. *Atmos. Environ.* **2003**, *37* (Supplement 2), 39−49.
(44) Howard, C. J.; Kumar, A.; Malkina, I.; Mitloehner, F.; Green, P. G.; Flocchini, R. G.; Kleeman, M. J. Reactive organic gas emissions from livestock feed contribute significantly to ozone production in central California. *Environ. Sci. Technol.* **2010**, *44*, 2309−14.
(45) *Guidance on the Use of Models and Other Analyses for Demonstrating Attainment of Air Quality Goals for Ozone, PM2.5, and Regional Haze*; United States Environmental Protection Agency: Research Triangel Park, NC, 2007.
(46) Rasmussen, D. J.; Fiore, A. M.; Naik, V.; Horowitz, L. W.; McGinnis, S. J.; Schultz, M. G. Surface ozone-temperature relationships in the eastern US: A monthly climatology for evaluating chemistry-climate models. *Atmos. Environ.* **2012**, *47*, 142−153.
(47) Rubin, J. I.; Kean, A. J.; Harley, R. A.; Millet, D. B.; Goldstein, A. H. Temperature dependence of volatile organic compound evaporative emissions from motor vehicles. *J. Geophys. Res.-Atmos.* **2006**, *111*.
(48) Baertsch-Ritter, N.; Keller, J.; Dommen, J.; Prevot, A. S. H. Effects of various meteorological conditions and spatial emission resolutions on the ozone concentration and ROG/NO_x limitation in the Milan area (I). *Atmos. Chem. Phys.* **2004**, *4*, 423−438.
(49) Pollack, I. B.; et al. Airborne and ground-based observations of a weekend effect in ozone, precursors, and oxidation products in the California South Coast Air Basin. *J. Geophys. Res.-Atmos.* **2012**, *117*, 2156−2202.
(50) Duncan, B. N.; Yoshida, Y.; Olson, J. R.; Sillman, S.; Martin, R. V.; Lamsal, L.; Hu, Y.; Pickering, K. E.; Retscher, C.; Allen, D. J.; Crawford, J. H. Application of OMI observations to a space-based indicator of NO_x and VOC controls on surface ozone formation. *Atmos. Environ.* **2010**, *44*, 2213−2223.
(51) Seinfeld, J. H.; Pandis, S. N. *Atmospheric Chemistry and Physics: From Air Pollution to Climate Change*, 2nd ed.; J. Wiley: Hoboken, N.J., 2006; p xxviii.
(52) Pusede, S. E.; Cohen, R. C. On the observed response of ozone to NO_x and VOC reactivity reductions in San Joaquin Valley California 1995 to present. *Atmos. Chem. Phys.* **2012**, *12*, 8323−8339.